Design of Pyridopyrazine-1,6-dione γ-Secretase Modulators that Align Potency, MDR Efflux Ratio, and Metabolic Stability

Martin Pettersson,*[†] Douglas S. Johnson,[†] John M. Humphrey,[‡] Todd W. Butler,[‡] Christopher W. am Ende,[‡] Benjamin A. Fish,[‡,§] Michael E. Green,[†] Gregory W. Kauffman,[‡] Patrick B. Mullins,[‡] Christopher J. O'Donnell,[‡] Antonia F. Stepan,[†] Cory M. Stiff,[‡] Chakrapani Subramanyam,[‡] Tuan P. Tran,[‡] Beth Cooper Vetelino,[‡] Eddie Yang,[‡] Longfei Xie,[‡] Kelly R. Bales,[†] Leslie R. Pustilnik,[‡] Stefanus J. Steyn,[†] Kathleen M. Wood,[†] and Patrick R. Verhoest[†]

[†]Pfizer Worldwide Research & Development, 610 Main Street, Cambridge, Massachusetts 02139, United States
[‡]Pfizer Worldwide Research & Development, Eastern Point Road, Groton, Connecticut 06340, United States

Ⓢ *Supporting Information*

ABSTRACT: Herein we describe the design and synthesis of a series of pyridopyrazine-1,6-dione γ-secretase modulators (GSMs) for Alzheimer's disease (AD) that achieve good alignment of potency, metabolic stability, and low MDR efflux ratios, while also maintaining favorable physicochemical properties. Specifically, incorporation of fluorine enabled design of metabolically less liable lipophilic alkyl substituents to increase potency without compromising the sp³-character. The lead compound **21** (PF-06442609) displayed a favorable rodent pharmacokinetic profile, and robust reductions of brain Aβ42 and Aβ40 were observed in a guinea pig time-course experiment.
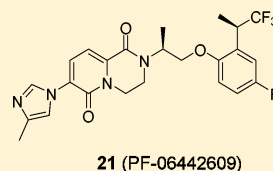
Aβ42 IC$_{50}$ = 6 nM
clogP = 3.1
LipE = 4.8
LipMetE = 2.0
HLM $CL_{int,app}$ = 12.7 mL/min/kg
MDR ER = 1.4

21 (PF-06442609)

KEYWORDS: *Alzheimer's disease, gamma secretase modulators, fluorine, lipophilic metabolism efficiency, LipMetE*

Alzheimer's disease (AD) is a progressive neurodegenerative disorder that is characterized by gradual loss of memory, impaired speech and motor functions, and is ultimately fatal. An estimated 5.2 million people currently suffer from AD in the US alone, and it is a major unmet medical need given the lack of disease modifying therapies to slow the progression of the disease.[1] Accumulation of brain amyloid plaques is a characteristic feature of AD pathology. These plaques consist primarily of the neurotoxic peptide amyloid β42 (Aβ42), which is formed via sequential cleavage of the amyloid precursor protein (APP) by β-secretase (BACE) and γ-secretase.[2] Development of compounds that inhibit or modulate these enzymes has therefore become a major focus in the search for disease modifying drugs.

γ-Secretase inhibitors (GSIs) have progressed to phase II and phase III clinical trials and demonstrated robust reduction of Aβ42 in human cerebrospinal fluid (CSF).[3] However, several adverse events were observed, such as gastrointestinal toxicity, increased occurrence of skin cancer, and negative effects on cognition.[4,5] These findings may in part be attributed to inhibition of Notch signaling, which is critical for cell differentiation.[6] It has also been hypothesized that accumulation of the C99 BACE cleavage product of APP could be a contributing factor to the cognitive decline.[7] In contrast to GSIs, γ-secretase modulators (GSMs) do not inhibit the proteolytic activity of γ-secretase, but rather shift the cleavage site of APP to reduce formation of Aβ42 and Aβ40, in favor of the shorter, less toxic species Aβ38 and/or Aβ37.[8,9] Development of GSMs has therefore emerged as a promising approach

for the treatment of AD. γ-Secretase is an intramembrane-cleaving aspartyl protease and is composed of at least four subunits; presenilin, nicastrin, Aph1, and Pen2.[10] Through the use of photoaffinity probes, we and others have demonstrated that several classes of GSMs bind to allosteric sites on presenilin that are distinct from the binding sites of GSIs.[11,12]
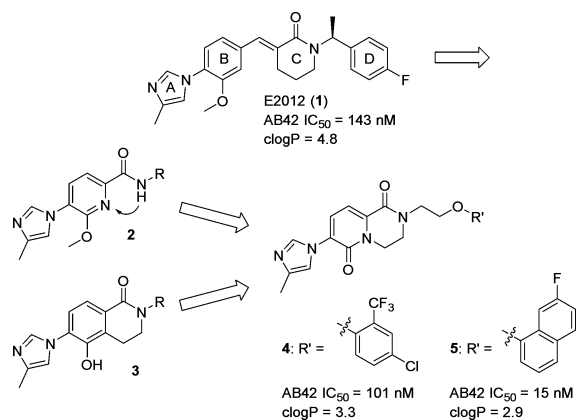
Examination of the patent literature points to significant challenges in identifying potent GSMs within favorable CNS physicochemical property space.[13] We have previously disclosed an amide series (generically represented by **2**) of GSMs using E2012 (**1**) as a scaffold (Scheme 1).[14−16] However, efforts to align potency (IC$_{50}$ < 100 nM) with adequate physicochemical properties and acceptable absorption, distribution, metabolism, and excretion (ADME) attributes were unfruitful in this series. Furthermore, stronger inhibition of cytochrome P450 enzymes (CYP450) was noted with more potent analogues. Our focus was therefore shifted toward designing novel, conformationally restricted cores with increased polarity.[17,18] As previously published, merging the hydroxy-substituted bicyclic core of **3** with pyridyl amide **2** afforded a novel pyridopyrazine-1,6-dione heterocyclic scaffold (i.e., **4** and **5**; Scheme 1) that maintained the key polar interactions required for potency but was devoid of liabilities associated with the phenol.[17]

Scheme 1. Evolution of the Pyridopyrazine-1,6-dione Series

Table 1. Activity of 9−14

	R	IC$_{50}$ (Aβ42, nM)[a]	cLogP	MDR ER[b]	HLM CL$_{int,app}$ (mL/min/kg)[c]
9		302	2.1	4.9	28.8
10		104	2.5	5.1	35.3
11		18	2.6	2.5	31.1
12		72	1.2	3.7	< 8
13		17	2.2	2.1	20.0
14		25	3.0	2.1	17.4

[a]Aβ42 IC$_{50}$ values were obtained in a whole cell assay using CHO APP$_{wt}$ cells. [b]MDR efflux ratio using a MDR1/MDCK assay utilizing MDCK cells transfected with the gene that encodes human P-glycoprotein.[26] [c]Human liver microsome-derived scaled intrinsic clearance.[23]

Development of robust, parallel enabled chemistry allowed for rapid optimization to afford pyridone 4,[17,19] which has moderate Aβ42-lowering activity in CHO APP cells (Aβ42 IC$_{50}$ = 101 nM) and favorable physicochemical properties: cLogP = 3.3,[20] central nervous system multiple parameter optimization score (CNS MPO) = 4.6,[21] and LipE = 3.9.[22] Compound 4 displayed dose-dependent reduction of brain Aβ42 in a guinea pig model, but additional gains in potency and in vivo efficacy were ultimately needed. Ongoing parallel chemistry efforts delivered naphthyl analogue 5, which displayed excellent in vitro activity while maintaining good properties (Aβ42 IC$_{50}$ = 15 nM; cLogP = 2.85). However, despite excellent human liver microsomal stability, this compound exhibited high turnover in rat liver microsomes (HLM CL$_{int,app}$ = 8.1 mL/min/kg; RLM CL$_{int,app}$ = 469 mL/min/kg), which complicates in vivo efficacy and safety studies in rodents.[23,24] Herein, we describe our efforts to optimize the pyridopyrazine-1,6-dione series to combine potency under 10 nM with good ADME profile and favorable physicochemical properties. The strategic use of fluorine played a key role in achieving these objectives.
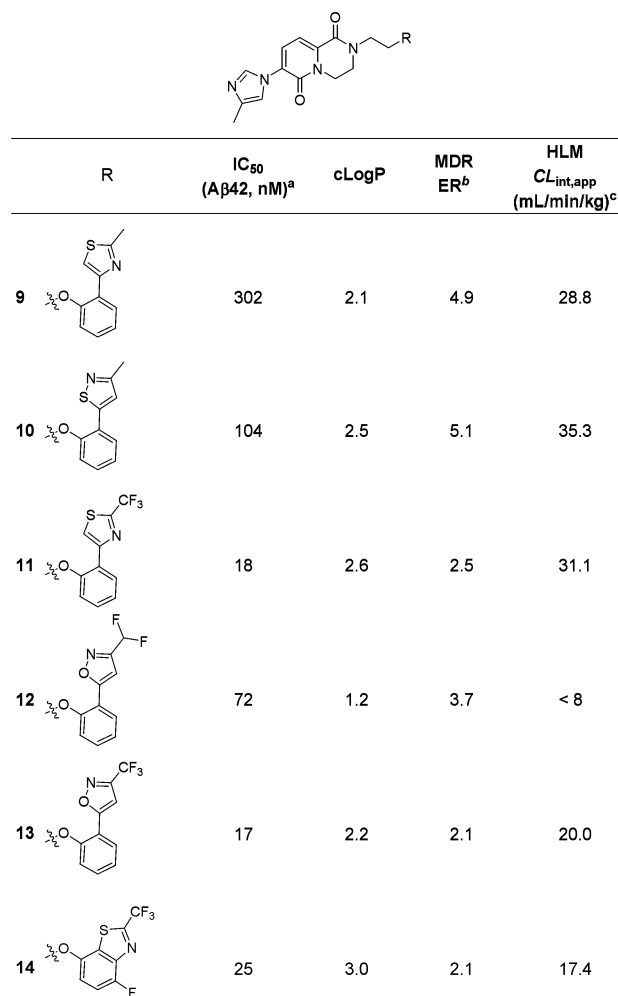
Through parallel medicinal chemistry using a previously developed protocol (Scheme 2), we sought to identify

Scheme 2. Synthesis of 9−13 and 15−21
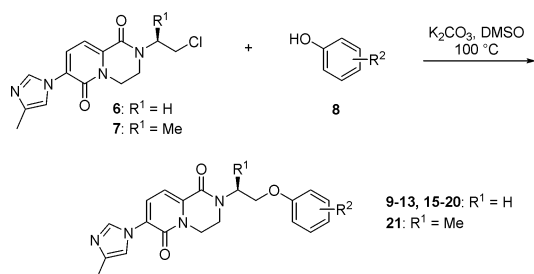
heterocyclic replacements for the naphthyl group of 5.[17,25] Several interesting compounds emerged such as thiazole 9 and isothiazole 10, which maintained moderate Aβ42-lowering activity (Table 1). However, consistent with previous observations, increased polarity in the right-hand section of the molecule came at the expense of high MDR efflux ratio (MDR ER).[26] To address this issue, we explored replacing the methyl group of 9 with an electron-withdrawing trifluoromethyl group to reduce the electron density of the heterocycle. This modification also had the potential to improve potency since we had previously observed a dramatic improvement in Aβ42-

lowering activity by replacing a methyl group with a trifluoromethyl substituent in this region of the molecule.[17]

The resulting analogue 11 achieved both design objectives; not only was the Aβ42 IC$_{50}$ improved from 302 to 18 nM, but the MDR ER was reduced from 4.9 to 2.5 while maintaining a cLogP value below 3.0. Similarly, library hit 12 incorporating a difluoromethyl-substituted isoxazole exhibited a promising in vitro profile. Using the same tactic of introducing a trifluoromethyl group, potency was improved from 72 to 17 nM (compound 13), and the MDR ER was reduced from 3.7 to 2.1 while maintaining good stability in human liver microsomes (CL$_{int,app}$ = 20.0 mL/min/kg). Finally, we explored a small set of targets designed specifically as naphthyl replacements. These efforts resulted in benzothiazole 14, which had potency approaching that of 5 while maintaining good ADME and properties (Aβ42 IC$_{50}$ = 25 nM, MDR ER = 2.1, and cLogP = 3.0).

The lead compounds were then evaluated in vivo to examine their pharmacokinetic (PK) profile. However, compounds 13 and 14 were found to have inadequate oral exposure when dosed in rat at 5 mg/kg even though RLM stability had been

improved relative to **5** (**5**, **13**, and **14** had RLM $CL_{int,app}$ = 469, 89.5, and 87.0 mL/min/kg, respectively). One concern with these compounds was the presence of four aromatic rings resulting in reduced sp^3-character.[27] The design strategy was therefore shifted to improve this parameter while maintaining good alignment of potency, physicochemical properties, and ADME profile. Re-examination of the library data revealed compounds with simple alkyl substituents in the ortho-position that maintained reasonable activity and that could serve as starting points for further optimization. Two of these included *t*-butyl analogue **15** and cyclobutyl compound **16**, which had Aβ42 IC$_{50}$ values of 128 and 73 nM, respectively (Table 2). Metabolic stability was poor, which may be expected given that the aliphatic substituents are susceptible to oxidative metabolism.

We hypothesized that clearance could be improved by introducing fluorine atoms to block potential sites of oxidative metabolism. Furthermore, incorporation of fluorine into this region would likely improve potency based on previous

structure−activity relationship (SAR) observations.[17] Toward this end, difluoro-substitution was installed on the cyclobutyl group of **16**, as well as an additional fluorine in the para-position of the phenol since we have previously shown that blocking this metabolic soft spot can lead to an improvement in both HLM and RLM stability.[17] The resultant compound **17** did indeed have significantly better metabolic stability (HLM $CL_{int,app}$ = 17.3 vs 93.8 mL/min/kg for **16**), but in vitro Aβ42-lowering activity was only marginally improved from 73 to 59 nM.
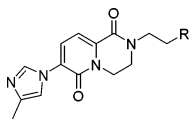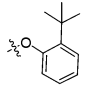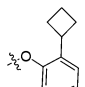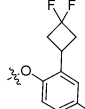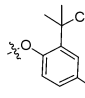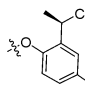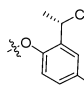
To increase potency and metabolic stability of **15**, one of the methyl groups of the *t*-butyl substituent was replaced with a trifluoromethyl group to afford **18**. The resultant 2,2-dimethyltrifluoroethyl moiety has previously been reported in the literature as a *t*-butyl replacement with improved metabolic stability.[29] As in the case of **17**, a fluorine atom was also introduced in the para-position of the right-hand aromatic ring to block this metabolically labile site. The resulting analogue **18** represented a significant advancement in that Aβ42-lowering activity was enhanced from 128 to 30 nM, and HLM stability was improved from 95.7 to 23.7 mL/min/kg while also maintaining low MDR ER and acceptable lipophilicity. The synthetic route to this custom phenol allowed ready access to the corresponding monomethyl analogues (i.e., **19** and **20**; see Supporting Information). Interestingly, removing one of the methyl groups of **18** followed by separation of enantiomers resulted in a further gain in potency and LipE. Compound **19** had an Aβ42 IC$_{50}$ value of 20 nM, whereas the enantiomer **20** was >4-fold less active. Metabolic stability was improved further, which is consistent with a reduction in cLogP. As shown in Table 2, fluorine appears to play a key role in improving the potency of **15** to ultimately deliver **19**; however, in the absence of an X-ray structure of γ-secretase, the nature of the specific molecular interactions remains unknown.

While compounds **11**, **13**, and **14** (Table 1) relied on a fourth aromatic ring to achieve good potency, incorporation of fluorine allowed successful design of potent GSMs such as **19** (Table 2) that have reduced aromatic ring-count and increased sp^3-character.[27] Specifically, incorporation of fluorine enabled the creation of lipophilic aryl-substituents with improved metabolic stability. Lipophilic metabolism efficiency (LipMetE) is a useful parameter to gauge metabolic stability at a given LogD (eq 1).[28] Higher LipMetE is preferable because it indicates that metabolic stability can be achieved within a wider LogD range. This is particularly relevant when pursuing an intramembrane target like γ-secretase, which may require higher lipophilicity to achieve sufficient potency and in vivo efficacy. As shown in Table 2, optimization of the *ortho*-alkyl substituent and incorporation of fluorine at specific sites led to significant improvements in metabolic stability while keeping lipophilicity relatively unchanged. This is reflected in an increase in LipMetE as exemplified by compounds **15** and **18**, which have LipMetE values of 0.9 and 1.8, respectively.[28]

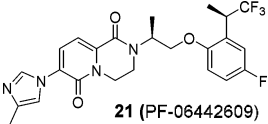$$LipMetE = LogD_{7.4} - Log_{10}(CL_{int,u}) \qquad (1)$$

While optimizing the terminal aryl ring we also explored introduction of conformational control elements on the methylene linker to orient the aryl ether into the putative hydrophobic pocket of the binding site. A methyl scan revealed that potency could be improved about 3-fold by introducing an S-methyl substituent as shown in **21** (Table 3; the corresponding R-enantiomer was 6-fold less active than **21**, not shown). Lead GSM **21** (PF-06442609)[30] represented a

Table 2. Activity of 15−20

	R	IC$_{50}$ (Aβ42, nM)[a]	cLogP	MDR ER[b]	HLM $CL_{int,app}$ (mL/min/kg)[c]	LipE[d] / LipMetE[e]
15	*t*-butyl phenyl ether	128	3.3	1.7	95.7	3.8 / 0.9
16	cyclobutyl phenyl ether	73	2.5	1.4	93.8	3.6 / 1.2
17	difluorocyclobutyl fluorophenyl ether	59	2.2	1.9	17.3	4.0 / 1.8
18	2,2-dimethyltrifluoroethyl fluorophenyl ether	30	3.2	1.8	24.3	3.5 / 1.8
19	(S)-trifluoroethyl fluorophenyl ether	20	2.8	1.7	12.3	4.4 / 1.8
20	(R)-trifluoroethyl fluorophenyl ether	85	2.8	1.7	23.4	3.9 / 1.4

[a]Aβ42 IC$_{50}$ values were obtained in a whole cell assay using CHO APPwt cells. Aβ42 IC$_{50}$ values are the geometric mean of at least two experiments. [b]MDR efflux ratio using a MDR1/MDCK assay utilizing MDCK cells transfected with the gene that encodes human P-glycoprotein.[26] [c]Human liver microsome-derived scaled intrinsic clearance.[23] [d]Lipophilic efficiency.[22] [e]Lipophilic metabolism efficiency.[28]

Table 3. Pharmacokinetic Parameters

21 (PF-06442609)

In Vitro Potency/Selectivity	
$A\beta 42$ IC_{50}	6 nM
NICD IC_{50}	>10 μM

Physicochemical Properties	
cLogP/SFLogD	3.1/3.4
LipE/LipMetE	4.8/2.0
CNS MPO	4.0
solubility (pH 6.5)[a]	101 μM

In Vitro ADME	
HLM $CL_{int,app}$	12.7 mL/min/kg
RLM $CL_{int,app}$	69.6 mL/min/kg
RRCK $P_{app,A \to B}$	16.0×10^{-6} cm/s
MDR ER	1.4

Rat PK	
B/P^{b}	0.8
$C_{b,u}/C_{p,u}{}^{b,c}$	0.4
CL^{d}	34.1 mL/min/kg
$T_{1/2}{}^{d}$	1.15 h
F^{e}	51%

[a]Kinetic solubility was measured at Analiza, Inc.[35] [b]Determined from 10 mg/kg oral dose, 1 h time point. [c]Plasma and brain free fractions of **21** in rat were 2.7% and 1.3%, respectively. [d]Determined from 1 mg/kg intravenous dose. [e]Calculated using the exposure from 1 mg/kg intravenous dose and 5 mg/kg oral dose.

major milestone in that single-digit potency ($A\beta 42$ IC_{50} = 6 nM) was successfully aligned with excellent microsomal stability, good passive permeability,[31] and low MDR efflux ratio (HLM $CL_{int,app}$ = 12.7 mL/min/kg; RRCK $P_{app,A \to B}$ = 16.0 $\times 10^{-6}$ cm/s;[31] MDR ER = 1.4) while maintaining favorable physicochemical properties (cLogP = 3.1; SFLogD = 3.4;[32] CNS MPO = 4.0). This is further highlighted by the fact that **21** has one of the highest LipE and LipMetE values of the compounds explored in this series (LipE = 4.8; LipMetE = 2.0). In addition to good HLM stability, **21** also had significantly improved stability in rat liver microsomes as compared to initial lead **5** (RLM $CL_{int,app}$ = 69.6 vs 469 mL/min/kg for **21** and **5**, respectively), which contributed to acceptable rat pharmacokinetic parameters (CL = 34.1 mL/min/kg; F = 51%; Table 3). In addition, **21** achieved good brain penetration in rat as indicated by a brain to plasma ratio (B/P) of 0.8 and an unbound brain to unbound plasma ratio ($C_{b,u}/C_{p,u}$) of 0.4. Finally, GSM **21** exhibited only moderate hERG activity (IC_{50} = 9.2 μM),[33] and it was devoid of Notch inhibition (NICD IC_{50} > 50 μM),[17] which is consistent with the desired profile of a GSM.

In vivo efficacy of **21** was evaluated in a guinea pig time-course experiment. Compound **21** was administered orally at a dose of 60 mg/kg, and $A\beta 42$, $A\beta 40$, $A\beta 38$, and $A\beta$-total were measured along with compound exposure at time-points ranging from 1 to 24 h. Sustained reductions of both $A\beta 42$ and $A\beta 40$ were achieved, while $A\beta$-total remained relatively unchanged (Figure 1). A 41% reduction of brain $A\beta 42$ was observed at the 3 h time-point for the 60 mg/kg dose, whereas
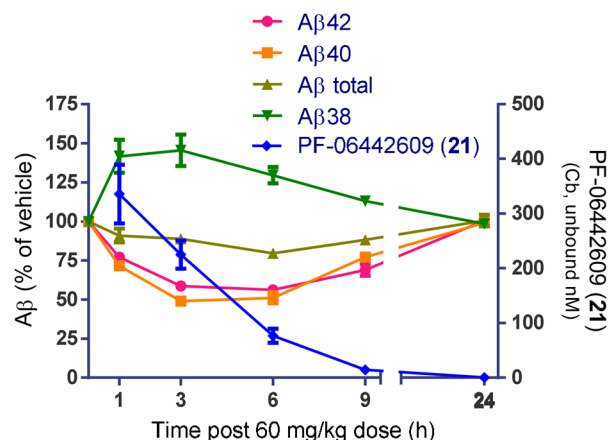

Figure 1. Guinea pig time course study.

$A\beta 38$ was increased 46% in accordance with the typical profile of a GSM. The corresponding unbound brain and plasma exposures at the 3 h time-point were 225 $\pm$ 45 and 680 $\pm$ 152 nM, respectively (see Supporting Information for further details on efficacy and exposure data).

While the initial synthesis of **21** (Scheme 2, using **7**) was adequate for producing milligram quantities for in vitro screening, it was not suitable for large scale synthesis to support in vivo studies. Steric bulk imparted by the 1,1,1-trifluoropropan-2-yl substituent resulted in a sluggish chloride displacement reaction that was accompanied by formation of a side product resulting from elimination of **7** rather than alkylation. This prompted our investigation into an alternative disconnection giving rise to amine **27** and lactone **29** (Scheme 3). This strategy offered a more convergent approach, allowing for C−O bond formation between phenol **25** and the readily available (S)-N-Boc-alaninol. The final step in generating **21** was envisioned as a lactone-to-lactam conversion utilizing this chiral amine.

Our synthesis of the requisite phenol **25** began with Suzuki coupling of commercially available boronic acid **22** with 2-bromo-3,3,3-trifluoropropene to afford the styrene derivative **23**. Demethylation of the methoxy group using BBr$_3$ afforded phenol **24**, and asymmetric catalytic hydrogenation with ([RuCl(p-cymene)(S)-Segphos)]Cl) delivered the chiral phenol **25** in excellent ee (96% ee; 72% yield).[34] Alkylation of **25** with (S)-N-Boc-alaninol methanesulfonate, followed by Boc deprotection and isolation of the amine as a solid fumarate salt completed the synthesis of amine **27**.

The highly crystalline lactone **29** was prepared from the known pyridone carboxylic acid **28**[17] via bis-alkylation with 1,2-dibromoethane. The amide **30** could then be obtained through simple amidation with **27** in hot methanol. However, to achieve acceptable conversion it was necessary to use superstoichiometric quantities (>3 equiv) of the precious amine **27**, which was undesirable for large scale synthesis. Instead, the amidation was more efficiently carried out using the Lewis acidic DABAL-Me$_3$ reagent to afford **30** in 72% yield. Lactam formation to generate the final target **21** was subsequently achieved in a one pot procedure through in situ generation of a mixed anhydride with trifluoroacetic anhydride followed by intramolecular alkylation of the amide by treatment with DBU.

We have described the design strategies and synthetic efforts leading to advanced GSM **21** using pyridopyrazine-1,6-dione leads **4** and **5** as starting points. Strategic use of fluorine played

Scheme 3. Synthesis of 21[a]
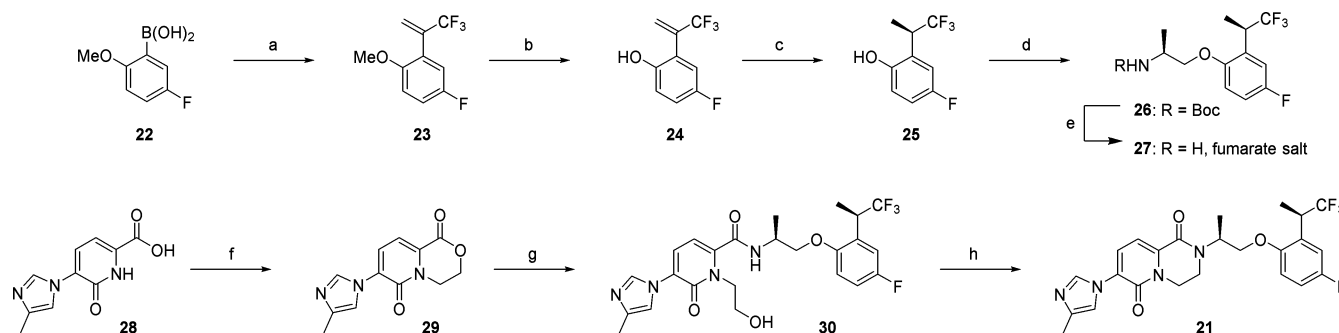
[a]Reagents and conditions: (a) 2-bromo-3,3,3-trifluoroprop-1-ene, $(PPh_3)_2PdCl_2$, K_2CO_3, THF, H_2O, rt, 70%; (b) BBr_3, CH_2Cl_2, −78 °C to rt, 74%; (c) 75 psi H_2, [RuCl(p-cymene)(S)-Segphos)]Cl, EtOH, 50 °C, 72%, 96% ee; (d) (S)-N-(t-butoxycarbonyl)alaninol methanesulfonate, Cs_2CO_3, DMF, 60 °C; (e) TFA, CH_2Cl_2, rt, then fumaric acid in MeOH, 78% (2 steps from **26**); (f) 1,2-dibromoethane, Cs_2CO_3, DMF, 90 °C, 76%; (g) **27**, DABAL-Me_3, THF, 70 °C, 72%; (h) TFAA (3.5 equiv), DBU (8 equiv), CH_3CN, 0 °C to rt, 85%.

a key role in aligning potency and ADME properties such as reducing the MDR efflux ratio for GSMs incorporating a heterocyclic D-ring. Specific introduction of fluorine also enabled creation of metabolically less liable lipophilic aryl substituents leading to superior in vitro potency and HLM stability while maintaining good physicochemical properties and increased sp^3-character. This is reflected in improved LipE relative to **4**: compounds **4** and **21** have whole-cell LipE values of 3.9 and 4.8, respectively. LipMetE was utilized to gauge progress with respect to metabolic stability by normalizing for changes in lipophilicity. Compound **21** had a LipMetE value of 2.0, which was the highest in the series and compares favorably to the initial t-butyl substituted library hit **15** (LipMetE = 0.9). Finally, **21** demonstrated good rodent brain penetration and oral bioavailability as well as robust in vivo Aβ42- and Aβ40-lowering in guinea pig. Additional efforts focused on further improving in vivo efficacy and reducing the efficacious plasma concentration will be disclosed in a future publication.

■ ASSOCIATED CONTENT

Ⓢ Supporting Information
Experimental data for compound synthesis and characterization, assay protocols, in vivo efficacy, and exposure data. This material is available free of charge via the Internet at http://pubs.acs.org.

■ AUTHOR INFORMATION

Corresponding Author
*Tel: (617) 395-0705. E-mail: martin.pettersson@pfizer.com.

Present Address
§1723 Dove Cottage Drive, Charlotte, North Carolina 28226, United States.

Notes
The authors declare no competing financial interest.

■ ACKNOWLEDGMENTS

■ REFERENCES

(1) Thies, W.; Bleiler, L. Alzheimer's disease facts and figures. *Alzheimers Dement.* **2013**, *9*, 208−245.

(2) Karran, E.; Mercken, M.; De Strooper, B. The amyloid cascade hypothesis for Alzheimer's disease: an appraisal for the development of therapeutics. *Nat. Rev. Drug Discovery* **2011**, *10*, 698−712.

(3) Bateman, R. J.; Siemers, E. R.; Mawuenyega, K. G.; Wen, G.; Browning, K. R.; Sigurdson, W. C.; Yarasheski, K. E.; Friedrich, S. W.; Demattos, R. B.; May, P. C.; Paul, S. M.; Holtzman, D. M. A γ-secretase inhibitor decreases amyloid-β production in the central nervous system. *Ann. Neurol.* **2009**, *66*, 48−54.

(4) De Strooper, B. Lessons from a failed γ-secretase Alzheimer trial. *Cell* **2014**, *159*, 721−726.

(5) Coric, V.; van Dyck, C. H.; Salloway, S.; Andreasen, N.; Brody, M.; Richter, R. W.; Soininen, H.; Thein, S.; Shiovitz, T.; Pilcher, G.; Colby, S.; Rollin, L.; Dockens, R.; Pachai, C.; Portelius, E.; Andreasson, U.; Blennow, K.; Soares, H.; Albright, C.; Feldman, H. H.; Berman, R. M. Safety and tolerability of the γ-secretase inhibitor avagacestat in a phase 2 study of mild to moderate Alzheimer disease. *Arch. Neurol.* **2012**, *69*, 1430−1440.

(6) Haapasalo, A.; Kovacs, D. M. The many substrates of presenilin/γ-secretase. *J. Alzheimer's Dis.* **2011**, *25*, 3−28.

(7) Mitani, Y.; Yarimizu, J.; Saita, K.; Uchino, H.; Akashiba, H.; Shitaka, Y.; Ni, K.; Matsuoka, N. Differential effects between γ-secretase inhibitors and modulators on cognitive function in amyloid precursor protein-transgenic and nontransgenic mice. *J. Neurosci.* **2012**, *32*, 2037−2050.

(8) Weggen, S.; Eriksen, J. L.; Das, P.; Sagi, S. A.; Wang, R.; Pietrzik, C. U.; Findlay, K. A.; Smith, T. E.; Murphy, M. P.; Bulter, T.; Kang, D. E.; Marquez-Sterling, N.; Golde, T. E.; Koo, E. H. A subset of NSAIDs lower amyloidogenic Aβ42 independently of cyclooxygenase activity. *Nature* **2001**, *414*, 212−216.

(9) Kounnas, M. Z.; Danks, A. M.; Cheng, S.; Tyree, C.; Ackerman, E.; Zhang, X.; Ahn, K.; Nguyen, P.; Comer, D.; Mao, L.; Yu, C.; Pleynet, D.; Digregorio, P. J.; Velicelebi, G.; Stauderman, K. A.; Comer, W. T.; Mobley, W. C.; Li, Y. M.; Sisodia, S. S.; Tanzi, R. E.; Wagner, S. L. Modulation of γ-secretase reduces β-amyloid deposition in a transgenic mouse model of Alzheimer's disease. *Neuron* **2010**, *67*, 769−780.

(10) De Strooper, B.; Iwatsubo, T.; Wolfe, M. S. Presenilins and γ-Secretase: Structure, Function, and Role in Alzheimer Disease. *Cold Spring Harb. Perspect. Med.* **2012**, *2*, a006304.

(11) Pozdnyakov, N.; Murrey, H. E.; Crump, C. J.; Pettersson, M.; Ballard, T. E.; am Ende, C. W.; Ahn, K.; Li, Y.-M.; Bales, K. R.; Johnson, D. S. γ-Secretase modulator (GSM) photoaffinity probes reveal distinct allosteric binding sites on presenilin. *J. Biol. Chem.* **2013**, *288*, 9710−9720.

(12) Crump, C. J.; Johnson, D. S.; Li, Y.-M. Development and mechanism of γ-secretase modulators for Alzheimer's disease. *Biochemistry* **2013**, *52*, 3197−3216 and references therein.

(13) Pettersson, M.; Stepan, A. F.; Kauffman, G. W.; Johnson, D. S. Novel γ-secretase modulators for the treatment of Alzheimer's disease: a review focusing on patents from 2010 to 2012. *Expert. Opin. Ther. Pat.* **2013**, *23*, 1349−1366.

(14) Pettersson, M.; Johnson, D. S.; Subramanyam, C.; Bales, K. R.; am Ende, C. W.; Fish, B. A.; Green, M. E.; Kauffman, G. W.; Lira, R.; Mullins, P. B.; Navaratnam, T.; Sakya, S. M.; Stiff, C. M.; Tran, T. P.; Vetelino, B. C.; Xie, L.; Zhang, L.; Pustilnik, L. R.; Wood, K. M.; O'Donnell, C. J. Design and synthesis of dihydrobenzofuran amides as orally bioavailable, centrally active γ-secretase modulators. *Bioorg. Med. Chem. Lett.* **2012**, *22*, 2906−2911.

(15) For related approaches, see Hall, A.; Patel, T. R. γ-Secretase modulators: current status and future directions. *Prog. Med. Chem.* **2014**, *53*, 101−145 and references therein.

(16) Gijsen, H. J.; Mercken, M. γ-Secretase modulators: can we combine potency with safety? *Int. J. Alzheimer's Dis.* **2012**, *2012*, 295207.

(17) Pettersson, M.; Johnson, D. S.; Subramanyam, C.; Bales, K. R.; am Ende, C. W.; Fish, B. A.; Green, M. E.; Kauffman, G. W.; Mullins, P. B.; Navaratnam, T.; Sakya, S. M.; Stiff, C. M.; Tran, T. P.; Xie, L.; Zhang, L.; Pustilnik, L. R.; Vetelino, B. C.; Wood, K. M.; Pozdnyakov, N.; Verhoest, P. R.; O'Donnell, C. J. Design, synthesis, and pharmacological evaluation of a novel series of pyridopyrazine-1,6-dione γ-secretase modulators. *J. Med. Chem.* **2014**, *57*, 1046−1062.

(18) Pettersson, M.; Johnson, D. S.; Humphrey, J. M.; am Ende, C. W.; Evrard, E.; Efremov, I.; Kauffman, G. W.; Stepan, A. F.; Stiff, C. M.; Xie, L.; Bales, K. R.; Hajos-Korcsok, E.; Murrey, H. E.; Pustilnik, L. R.; Steyn, S. J.; Wood, K. M.; Verhoest, P. R. Discovery of indole-derived pyridopyrazine-1,6-dione γ-secretase modulators that target presenilin. *Bioorg. Med. Chem. Lett.* **2015**, *25*, 908−913.

(19) Tran, T. P.; Mullins, P. B.; am Ende, C. W.; Pettersson, M. Synthesis of pyridopyrazine-1,6-diones from 6-hydroxypicolinic acids via a one-pot coupling/cyclization reaction. *Org. Lett.* **2013**, *15*, 642−645.

(20) Values for cLogP were calculated using the BIOBYTE (www.biobyte.com) program cLogP, version 4.3.

(21) Wager, T. T.; Hou, X.; Verhoest, P. R.; Villalobos, A. Moving beyond rules: the development of a central nervous system multiparameter optimization (CNS MPO) approach to enable alignment of druglike properties. *ACS Chem. Neurosci.* **2010**, *1*, 435−449.

(22) LipE = −log(EC$_{50}$) − LogD where EC$_{50}$ is in molar units and LogD was experimentally determined using shake flask LogD.[32] For additional detail, see Ryckmans, T.; Edwards, M. P.; Horne, V. A.; Correia, A. M.; Owen, D. R.; Thompson, L. R.; Tran, I.; Tutt, M. F.; Young, T. Rapid assessment of a novel series of selective CB(2) agonists using parallel synthesis protocols: a lipophilic efficiency (LipE) analysis. *Bioorg. Med. Chem. Lett.* **2009**, *19*, 4406−4409.

(23) Assay method adapted from published protocols: Riley, R. J.; McGinnity, D. F.; Austin, R. P. A unified model for predicting human hepatic, metabolic clearance from in vitro intrinsic clearance data in hepatocytes and microsomes. *Drug. Metab. Dispos.* **2005**, *33*, 1304−1311.

(24) Obach, R. S. Prediction of human clearance of twenty-nine drugs from hepatic microsomal intrinsic clearance data: An examination of in vitro half-life approach and nonspecific binding to microsomes. *Drug. Metab. Dispos.* **1999**, *27*, 1350−1359.

(25) Compound **14** was not prepared via the alkylation route in Scheme 2, but rather using the HATU-mediated coupling/cyclization as previously published. See Pfizer WO 2012/131539.

(26) Feng, B.; Mills, J. B.; Davidson, R. E.; Mireles, R. J.; Janiszewski, J. S.; Troutman, M. D.; de Morais, S. M. In vitro P-glycoprotein assays to predict the in vivo interactions of P-glycoprotein with drugs in the central nervous system. *Drug. Metab. Dispos.* **2008**, *36*, 268−275.

(27) Lovering, F.; Bikker, J.; Humblet, C. Escape from flatland: increasing saturation as an approach to improving clinical success. *J. Med. Chem.* **2009**, *52*, 6752−6756.

(28) LipMetE was calculated using measured shake flask LogD[32] and unbound intrinsic clearance ($CL_{int,u}$) derived from the intrinsic apparent clearance ($CL_{int,app}$) and calculated human liver microsomal binding values. For additional details see Stepan, A. F.; Kauffman, G. W.; Keefer, C. E.; Verhoest, P. R.; Edwards, M. Evaluating the differences in cycloalkyl ether metabolism using the design parameter "lipophilic metabolism efficiency" (LipMetE) and a matched molecular pairs analysis. *J. Med. Chem.* **2013**, *56*, 6985−6990.

(29) Tanaka, H.; Shishido, Y. Synthesis of aromatic compounds containing a 1,1-dialkyl-2-trifluoromethyl group, a bioisostere of the tert-alkyl moiety. *Bioorg. Med. Chem. Lett.* **2007**, *17*, 6079−6085.

(30) Compound **21**, also known as PF-06442609, is now commercially available from Sigma Aldrich; catalog #PZ0258.

(31) Callegari, E.; Malhotra, B.; Bungay, P. J.; Webster, R.; Fenner, K. S.; Kempshall, S.; LaPerle, J. L.; Michel, M. C.; Kay, G. G. A comprehensive non-clinical evaluation of the CNS penetration potential of antimuscarinic agents for the treatment of overactive bladder. *Br. J. Clin. Pharmacol.* **2011**, *72*, 235−246.

(32) Shake flask LogD. Assay method adapted from published protocol: Hay, T.; Jones, R.; Beaumont, K.; Kemp, M. Modulation of the partition coefficient between octanol and buffer at pH 7.4 and pKa to achieve the optimum balance of blood clearance and volume of distribution for a series of tetrahydropyran histamine type 3 receptor antagonists. *Drug Metab. Dispos.* **2009**, *37*, 1864−1870.

(33) Kutchinsky, J.; Friis, S.; Asmild, M.; Taboryski, R.; Pedersen, S.; Vestergaard, R. K.; Jacobsen, R. B.; Krzywkowski, K.; Schroder, R. L.; Ljungstrom, T.; Helix, N.; Sorensen, C. B.; Bech, M.; Willumsen, N. J. Characterization of potassium channel modulators with QPatch automated patch-clamp technology: system characteristics and performance. *Assay Drug Dev. Technol.* **2003**, *1*, 685−693.

(34) RuCl(*p*-cymene)(*R*)-dm-segphos)Cl, CAS [944451−30−3].

(35) Solubility was measured by Analiza, Inc., Cleveland, OH (http://analiza.com/physchem/logd.html#qf).